FIRE PROTECTION & SAFETY Scientific Journal
16(2): 7–14, 2022
DOI: 10.17423/delta.2022.16.2.110

Comparison of the sensitivity of the FDS computational grid

Dorota Hodúlová [1*], Stanislava Gašpercová [1], Martin Dolnický [2]

[1] University of Žilina, Faculty of Security Engineering, Department of Fire Engineering; 1. mája 32, 010 26 Žilina, Slovakia; dorota.hodulova@uniza.sk; stanislava.gaspercova@uniza.sk

[2] Fire and Rescue Service Žiar nad Hronom; martin.dolnicky@gmail.com

[*] Corresponding author: dorota.hodulova@uniza.sk

Original scientific paper

Received: September 16, 2022; Accepted: September 29, 2022; Published: December 31, 2022

Abstract

The main objective of the paper is to assess the sensitivity of the selected CFD fire model as a function of the computational grid density in three separate simulations of a fire in a simple confined space. The selected fire model is the FDS program, which is used to model confined space fires and to track the fluid flow driven by the fire. The density sensitivity of the computational grid is assessed based on the values obtained for heat release rate, heat flux, space temperature, and smoke layer height. From these outputs, graphs of the evolution over time are produced, and finally, the individual outputs of each computational grid are compared and evaluated as a function of the accuracy of the output data and the speed of the simulations. The contribution of the paper is the determination of the optimal cell size of the computational grid concerning the complexity of the simulation duration.

Keywords: FDS; modelling fires; sensitivity of the computational grid

1 Introduction

Today we are experiencing rapid developments in all areas of life, which, in addition to new opportunities and possibilities, also bring with them many risks that need to be eliminated to protect persons and property. In particular, the construction industry has also made great progress in recent times, with ever larger and more complex buildings being constructed and occupied by large numbers of people. A fire in confined spaces is one of the main causes of danger to persons and property in these buildings. To protect against fires, it is necessary to have effective fire prevention measures in place, which also requires sufficient knowledge of the origin and spread of fire, which is conditioned by various parameters. These parameters can limit or intensify the fire and therefore the course of the fire is the subject of long-term research, supported by the development of technologies to ensure the safety of construction objects at risk of fire. This paper aims to create three simple space simulations in the FDS (Fire Dynamics Simulator) program and to assess the selected output data as a function of the computational grid density in the evolution of heat release rate, room temperature, smoke layer height and heat flux recorded from floor to ceiling.

2 Modelling of fires

Among the technology used to assess buildings for fire safety, we include fire models, which, thanks to scientific advances, are coming to the fore and are a common part of fire engineering. According to the STN (Slovak Technical Standard), a fire model is a fire design, based on a limited area of application of specific physical parameters, which is used to design fire safety of buildings, to assess the possibility of evacuation of the building, to create designs for heat dissipation devices with products of combustion, to design the location of fire detectors, to investigate the causes of fire

and its course and to analyze the risk of the building or operation. The distribution of fire models is shown in Fig. 1 [1, 2].

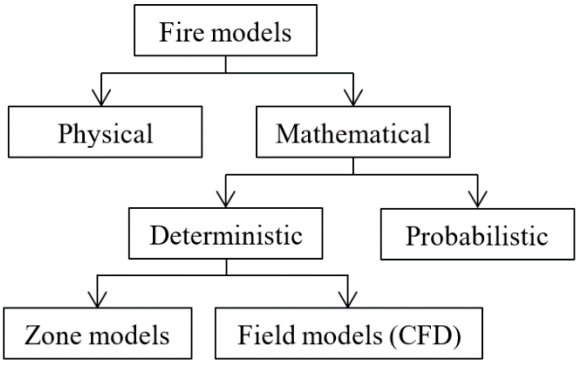

Fig 1. Fire models [3]

CFD (Computational Fluid Dynamics) is a fire model that allows the simulation of fluid motion in space. This type of model is classified as a deterministic fire model, which means that the space in which the fire is modelled is first plotted in the program. These models operate on the principle of a computational grid that divides the space into a large number of small computational cells, with the conservation laws of mass, momentum, energy, and the Navier-Stokes equation applying to each cell [4, 5].

For the use of the program in fire engineering, the program must be flexible and reliable. Flexibility is conditioned by the modernisation of the program depending on the advancement of technology and knowledge in the field. Reliability means the ability to model fires in complex spaces involving a large number of physical parameters. The reliability of the programme also depends on the number of cells contained in the computational grid, the higher the number of cells, the more detailed and accurate the outputs of heat flow, fire and smoke propagation. The CFD fire model is shown in Fig. 2 [5 - 7].

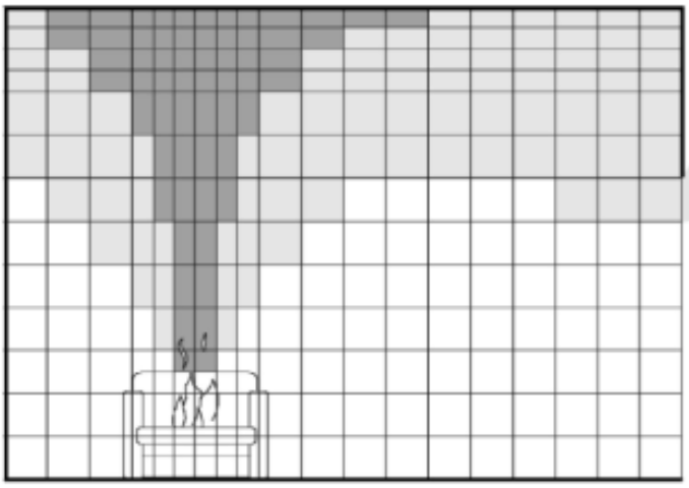

Fig 2. CFD fire model [4]

FDS is one of the most widely used software for the simulation of confined space fires, which is included in CFD models. FDS mainly focuses on the transport of heat and combustion products in a fire compartment with low fluid flow velocities. It is used to simulate thermal radiation, pyrolysis of solid and liquid, flame propagation of low-velocity heat and smoke flow, fire development and fire suppression [6, 8, 9].

FDS works as a set of several subroutines that express quantities and phenomena using mathematical equations, and then apply these calculations to each cell of the computational network

separately. The FDS program also includes the Smokeview program, which is used to visualize the obtained simulation results, which are three-dimensional, and has a colour scale that is used to represent the temperature differences, as shown in Fig. 3 [6, 8, 10].

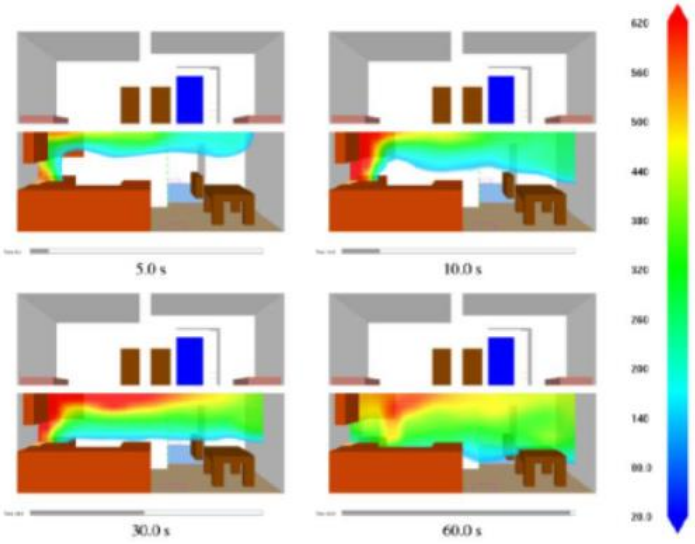

Fig 3. Fire visualisation in Smokeview [11]

3 Material and Methods

For the need to assess the sensitivity of the FDS program to the cell density of the computational grid, it will be necessary to create a simulation room of smaller dimensions with simple space geometry, as more complicated spaces and more complex simulations are very computationally intensive and require longer simulation times, even several days. When considering room dimensions, the dimensions of rooms (e.g. living room) in real life were also taken into account. Based on these factors, the dimensions of the computational grid for each of the three scenarios were chosen to be the same, x (width) = 5 m, y (length) = 4 m, and z height = 3 m, in which the density of cell placement was varied. The cell density of the computational grid was created based on the formula for calculating the optimal grip density D^* [8].

$$D^* = \left(\frac{Q}{\rho_\infty c_\infty T_\infty \sqrt{g}}\right)^{\frac{2}{5}} \quad (1)$$

Where D^* is the optimum grid density
Q is heat released in a fire
ρ is air density
c is the specific heat capacity of the air
T is the thermodynamic ambient air temperature
g is the gravitational acceleration

The values of the input parameters to formula (1) are given in Tab. 1. Those values were selected based on the definition of the simulation space, the size of the fire and the tabulated values according to [12].

Tab. 1 The values of the input parameters

Parameter	Value	Unit
Q	1 000	kW
ρ	1,204	$kg.m^3$
c	1,005	kJ/(kg.K)
T	293	K
g	9,81	$m.s^2$
D*	0,959	m

After calculating the size parameter D* = 0.959 m, the dimensions of the computational grid were determined. According to [8], the rule of thumb of using a suitable parameter to calculate the D* parameter is applied, which is divided by a factor of 5 to 20. Tab. 2 shows the grid sizes for the different scenarios with the conversion value.

Tab. 2 Cell dimensions of computational grids

Type of computational grid	Parameter of calculation	Calculated cell size	Cell size after rounding
Rough (Scenario 3)	5	0,1918 m	0,2 m
Medium (Scenario 2)	10	0,0959 m	0,1 m
Fine (Scenario 1)	20	0,0479 m	0,05 m

Once the simulation grids were created, objects and holes were created to create the simulation space. First, a 20 cm thick wall of concrete material was created. The opening in the wall, representing the door, was 80 cm wide and 2 m high. Next, a seating structure was constructed, which was placed against the back wall of the room, in the centre of the y-axis. The furniture is made of Upholstery material, which consists of Foam (10 cm) and Fabric (0.2 cm). To ventilate the room during the fire simulation, the space to the right of the wall, which is characterized by the Vent command, was used. The simulation room for each of the three scenarios was identical and is shown in Fig. 4.

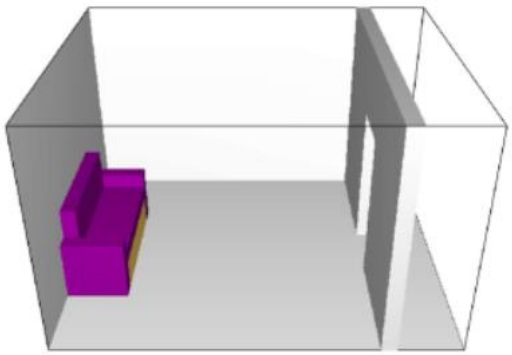

Fig 4. Visualizing the space in Smokeview

The source of initiation in the simulations was defined by the two hot particles of the *Ignitor Particle* commands, which were located in the upper corner of the seating furniture. To define these particles, a new *Ignitor surface* of type *Heater/Cooler* had to be created, which had a constant temperature set to 1 000 °C. Subsequently, a combustion reaction was defined through the substance undergoing thermal decomposition to form products of combustion and heat release. The fuel of the fire was polyurethane, which has a critical temperature of 1 327 °C.

As mentioned earlier, the paper focuses on comparing the outputs of the evolution of *Heat Release Rate*, *Heat Flux*, *Space Temperature* and *Smoke Layer Height* in three simulations. To obtain the outputs of the selected fire parameters, it was necessary to create devices in the FDS to record the results. The simulation length was set to 800 s, given that several variations of simulations were created, and a time of 800 s was the most acceptable given the length of the simulation and the relevance of the results.

4 Results

All the outputs obtained from the simulations were recorded in Microsoft Excel. The first simulation output that can be compared and evaluated is the simulation length. For *Scenario 1* the simulation took 98.5 minutes, for *Scenario 2* it was 8.4 hours and for *Scenario 3* 40 hours.

The first simulation output compared is the *Heat Release Rate*, the evolution plot of which is shown in Fig. 5.

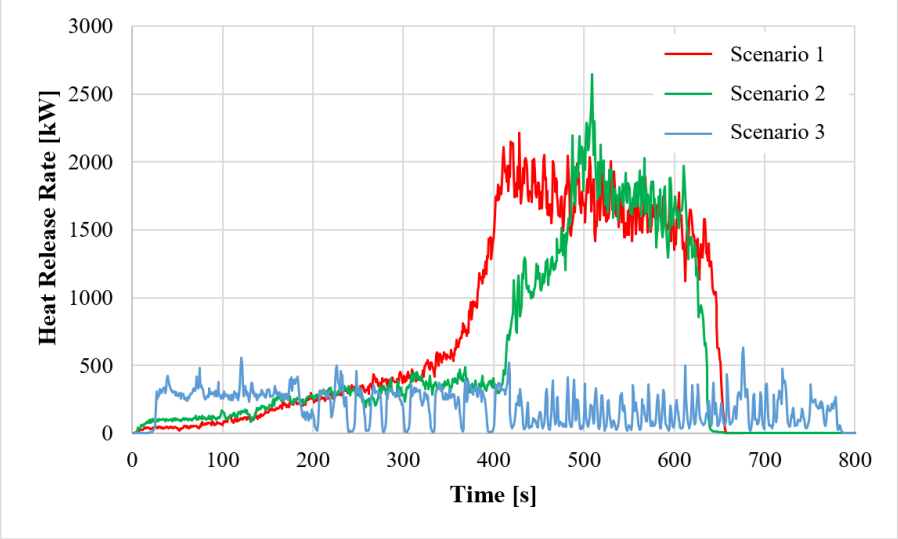

Fig 5. Comparison of Heat Release Rates of different scenarios

From the graph, it can be seen that the values of the *Heat Release Rate* evolution are very similar for *Scenario 1* and *Scenario 2*. First, for both scenarios the *Heat Release Rate* values increase linearly. Later in *Scenario 1*, there is a sharp increase at time 355.2 s, which continues until time 428.8 s, where the curve reaches a local maximum with a value of 2 210.01 kW. In *Scenario 2*, a sharp increase occurs later, at time 408 s, until at time 508.81 s the curve reaches a local maximum with a value of 2 643.25 kW. After reaching the local maximum, both curves start to slowly decrease until the complete cessation of burning, which is at time 676 s in *Scenario 1*, and at time 669.1 s in *Scenario 2*. In *Scenario 3*, the evolution of the *Heat Release Rate* is quite different, the curve fluctuates continuously until the cessation of the fire at 796.05 s. The local maximum in *Scenario 3* is reached at time 676.01 s with a value of 633.66 kW.

Another fire parameter investigated was the *Heat Flux*, the curves of which are shown in Fig. 6.

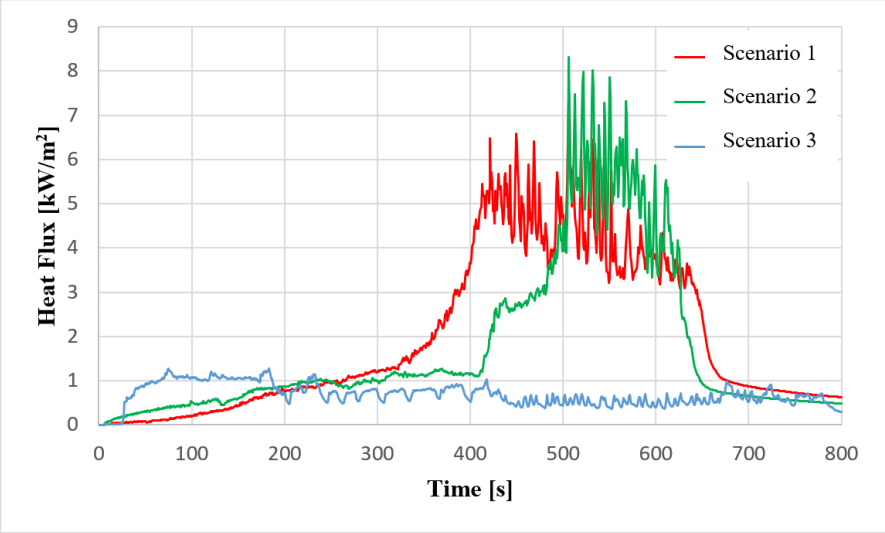

Fig 6. Comparison of Heat Fluxes of individual scenarios

Also for this examined parameter, the values of *Scenario 1* and *Scenario 2* are similar, and *Scenario 3* differs. The *Heat Flux* curves are similar to the *Heat Release Rate* curves. For *Scenario 1*, there is a sharp increase in *Heat Flux* at time 321.6 s, with a maximum value of 7.52 kW/m^2 reached at time 506.4 s, then there is a sharp decrease in *Heat Flux*, and after time 672.8 s this decrease is linear. The curve of *Scenario 2* is very similar, the sharp increase in *Heat Flux* occurs later, at 414.4 s, and the maximum is reached at 506.4 s at 8.31 kW/m^2. After the maximum value is reached, there is a sharp exponential decrease in the *Heat Flux*, and from time 659.22 s onwards a linear decrease until the fire stops. The curve of *Scenario 3* is again quite different with a large number of fluctuations, the maximum value of the *Heat Flux* reached is 1.27 kW/m^2 at time 75.2 s.

To compare the sensitivity of the computational grid, we can also compare the *Space Temperature* which is shown in Fig. 7.

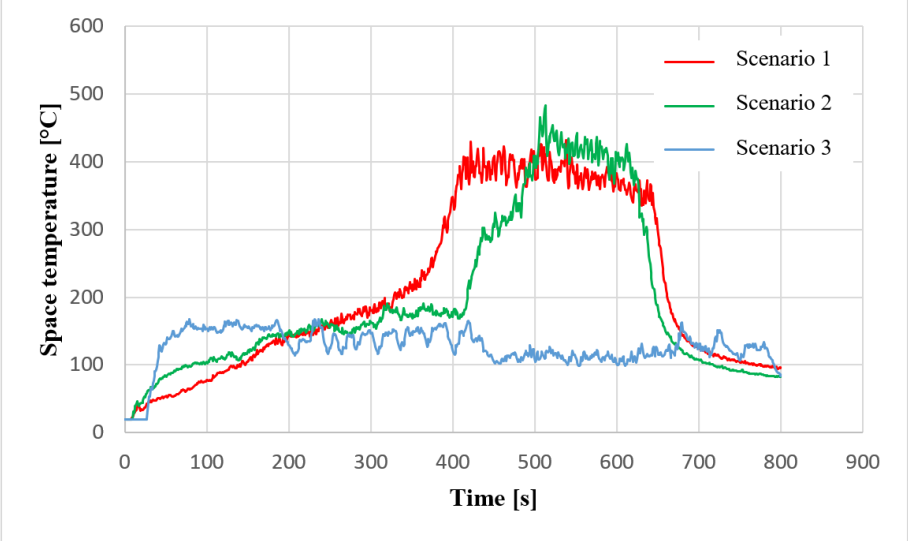

Fig 7. Comparison of Space Temperature in different scenarios

From the evolution of the *Space Temperature* curves, it is evident that they follow the *Heat Flux* curves. Again, the *Scenario 1* and *Scenario 2* curves are very similar, while at the same time quite different from *the Scenario 3* curve. The maximum *Space Temperature* reached among all scenarios is

483 °C, which means that no Flashover has occurred in the simulation space, as the conditions for its occurrence are not met.

The last graph, Pic. 8, shows the evolution of the change of the *Smoke Layer Height* over time.

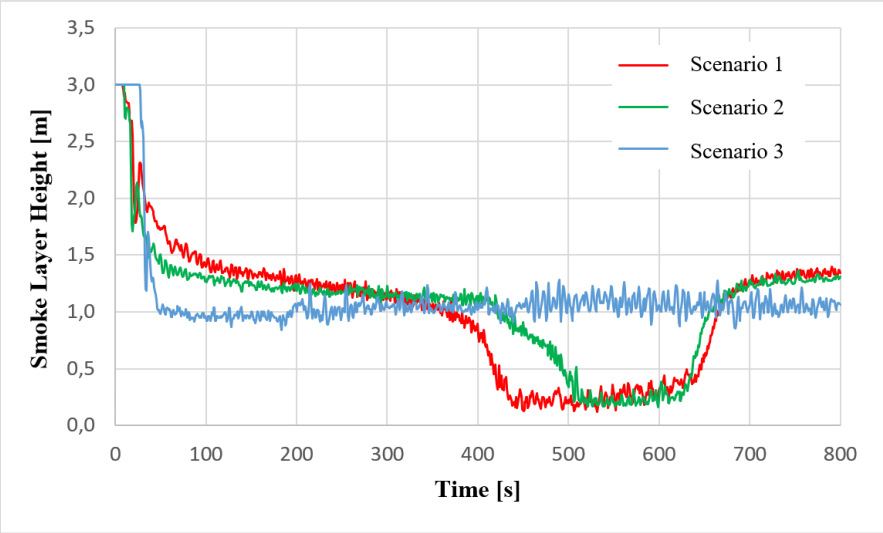

Fig 8. Comparison of Smoke Layer Height in different scenarios

As with the previous parameters, the *Smoke Layer Height* and *Scenario 1* and *Scenario 2* curves are almost identical, but in this case the *Scenario 3* curve is not so different. The ceiling height in the fire room is 3 m. The *Smoke Layer Height* is approximately the same in all three scenarios, until 33 s when there is a gradual divergence. The minimum reached *Smoke Layer Height* for *Scenario 1* is 0.12 m above the floor at time 644 s. For *Scenario 2* it is 0.16 m at time 642 s and for *Scenario 3* it is 0.84 m at time 127 s. At the end of the fire, the curves of *Scenario 1* and *Scenario 2* are almost identical and the *Smoke Layer Height* is rising. *For Scenario 3*, the value of the *Smoke Layer Height* remains approximately the same until the end of the fire.

5 Discussion and conclusions

The above graphs show that the outputs of *Scenario 1* and *Scenario 2* are very similar in all parameters examined. For the *Heat Release Rate*, the maximum values are different mainly in the times of their attainment, namely 428.8 s and 508.81 s. For the *Heat Flux* values, the difference is again observed mainly in the times of their attainment, but the maximum values attained are different only by 0.79 kW/m2. For the *Smoke Layer Height*, the curves are again very similar and differ only in the times of the maximum smoke plume in the space.

It is generally known that computational grids with larger dimensions do produce not very accurate results, but their duration is the shortest of all. Conversely, computational grids with smaller cell sizes achieve very accurate results, but their simulation duration exceeds several days, even weeks, depending on the complexity of the model situation. Based on these findings, and comparing them with the simulations, we see that *Scenario 3*, differs very significantly from *Scenario 1* and *Scenario 2*. The observed results of *Scenario 3* are not even consistent with the generally known fire scenario. The results of *Scenario 1* and *Scenario 2* follow the trend of the generally known fire behaviour. Therefore, it can be said that computational grids with smaller cell sizes are more suitable for fire simulations as their results are more accurate. Considering the duration of the simulations, the most acceptable variant of the computational cell sizes is *Scenario 2*, as its simulation length is not too restrictive, especially if we want to obtain accurate results in a short time. Based on simulations, we can assess that the parameter for the optimum density of the calculating distance D* could range from 10 to 20.

These obtained results show that the cell density of the computational grid has a great influence on the duration of the simulation. Considering the time, it is most advantageous to use a coarser distribution of computational grid cells in the simulations, however, the accuracy of the results, which is best obtained with finely spaced computational grid cells, will pay the price.

References

[1] STN EN 1991-1-2 (73 0035): 2007: Eurokód 1. Zaťaženia konštrukcií. Časť 1-2: Všeobecné zaťaženia. Zaťaženia konštrukcií namáhaných požiarom. 2007

[2] Kačíková D. 2013. Dynamika požiaru . (10 December 2022; http://www.gitech.sk/fire/images/dokumenty/Dynamika_poziaru.pdf)

[3] Cote AE. (Ed.). 2003. Fire Protection Handbook. 19th ed. National Fire Protection Association, Quincy, Mass

[4] Karlsson B, Quintiere JG. 2000. Enclosure fire Dynamics. FL: CRC Press

[5] Clarson J. 1999. Fire modelling using CFD. (10 December 2022; https://lup.lub.lu.se/luur/download?func=downloadFile&recordOId=1767130&fileOId=1770040)

[6] McGrattan K. 2022. Computational Fluid Dynamics modelling of fire, International Journal of Computational Fluid Dynamics. (10 December 2022; https://www.tandfonline.com/doi/full/10.1080/10618562.2012.659663)

[7] Razdolsky L. 2009. Mathematical Modeling of fire Dynamics

[8] Wald F. (Ed.). 2017. Modelování dynamiky požáru v budovách. Nakladatelství ČVUT

[9] Valášek L. 2014. Počítačová simulácia požiarov. Ústav informatiky SAV. (10 December 2022; https://www.math.sk/mpm/wp-content/uploads/2017/11/Seminar_Valasek.pdf)

[10] Forney G. 2022. Smokeview, A Tool for Visualizing Fire Dynamics Simulation Data Volume II: Technical Reference guide. (10 December 2022; https://pages.nist.gov/fds-smv/manuals.html)

[11] Forney G. 2022. Smokeview, A Tool for Visualizing Fire Dynamics Simulation Data Volume I: User´s Guide. (10 December 2022; https://pages.nist.gov/fds-smv/manuals.html)

[12] Chyský J. (Ed.). 1993. V*ě*trání a klimatizace. Nakladatelství BOLIT-B Press